International Journal of GEOMATE, July, 2017, Vol.13, Issue 35, pp.166 - 173
Geotec., Const. Mat. & Env., ISSN:2186-2990, Japan, DOI: http://dx.doi.org/10.21660/2017.35.78775

FATIGUE RESISTANCE OF SURFACE TEMPERATURE REDUCING PAVEMENT UNDER FIXED-POINT LOAD

Hiroshi Higashiyama[1] and Masanori Sano[2]

[1]Faculty of Science and Engineering, Kindai University, Japan; [2]Research Institute for Science and Technology, Kindai University, Japan

*Corresponding author, Received: 22 Dec. 2016, Revised: 30 Jan. 2017, Accepted: 22 Feb. 2017

ABSTRACT: Asphalt and concrete pavements cover a high percentage of urban area. In the summer season, the surface temperature of asphalt pavements exposed to the solar radiation increases to 60°C or more. This is one cause of the urban heat island phenomenon. In the field of road engineering, cool pavements have been constructed to decrease the surface temperature and to improve the road environment. We have previously studied the cement-based grouting material containing cement, ceramic waste powder, and natural zeolite for cool pavements. This cool material is poured into voids in porous asphalt pavements. The construction method for this cool pavement is the same as that for water retaining pavements. The temperature measurements show that the surface temperature was lower by 15-20°C than the conventional porous asphalt pavement temperature of 60°C. On the other hand, the accumulation of permanent strain in the asphalt pavements causes rutting under passing traffic loads in the hot summer season. In this study, the fatigue tests under a fixed-point load were conducted to evaluate the fatigue resistance of the surface temperature reducing pavement at 40°C. The fatigue resistance of pavements under various loading levels is evaluated at sinking displacements of 15 and 20 mm. The test results show that the surface temperature reducing pavement has a higher fatigue resistance than conventional porous asphalt pavements.

Keywords: Cool pavement, Cement-based grouting material, Fatigue resistance, Fixed-point load

1. INTRODUCTION

Asphalt and concrete pavements cover a high percentage of urban area and largely affect development of the heat island phenomenon. In the field of road engineering, countermeasures against the heat island phenomenon are cool pavements that have been constructed in the urban areas to decrease the surface temperature and to improve the road environment [1], [2]. The authors have investigated cool pavements, like water retaining pavements. In the previous studies, a cool pavement was developed by using ultra-rapid hardening cement, ceramic waste powder, and natural zeolite. The outdoor measurements show that the cool pavement reduced the surface temperature by 15-20°C in comparison with the conventional porous asphalt pavement at 60°C in the hot summer [3], [4].

On the other hand, the permanent deformation of asphalt pavements such as rutting seriously affects the driving safety of traffic vehicles. The permanent deformation is the accumulated strain caused by passing traffic loads over time [5]. A higher resistance to such permanent deformation increases the fatigue life of asphalt pavements [6]. Many studies have been conducted with different test methods such as the three or four-point bending fatigue tests under controlled strain [7]-[9], the wheel-tracking tests [9], [10], and the single penetration repeated shear tests [6] to determine the fatigue life of asphalt mixtures.

The aim of this study is to evaluate the fatigue resistance of the cool pavement developed by the authors. In this study, the fatigue tests under a fixed-point load with different loading levels were carried out in water at 40°C for cool pavements and for conventional porous asphalt pavements. The fatigue life up to a certain sinking displacement at the loading point, which was regarded as a rutting depth, was compared with that of the conventional porous asphalt pavements.

2. EXPERIMENTAL PROGRAMS

2.1 Cement-based grouting material

The cement-based grouting material was prepared using ultra-rapid hardening cement (UHC), ceramic waste powder (CWP), and natural zeolite (NZ). The ceramic waste powder, which was collected in the recycling process of ceramic waste porcelain insulators, was supplied from the Kanden L&A Co., Ltd, Japan. The natural zeolite with a particle size of less than 200 μm was mined in Izumo, Shimane, Japan. The chemical and physical properties are shown in Table 1. The mixing ratio of UHC, CWP, and NZ was 0.5:0.35:0.15 by weight. The water-to-cement ratio (w/c) was kept constant at 1.3 by weight. To

increase the workability of the cement-based grouting material and the labor time during infiltration into porous asphalt pavements, an air entraining and high-range water reducing agent supplied from BASF Japan Ltd., Japan and a setting retarder were added by 3% and 0.4% of the UHC by weight, respectively [3], [4].

The flow value, which is evaluated by the falling flow time, measured by a method using a P-type funnel with a volume of 1725 ml according to JSCE-F 521 [11] was 9.34 s after the mixing of the cement-based grouting material finishes. This value is within the range of flow times of 9 to 13 s recommended by road constructors in Japan. The compressive strength development of the cement-based grouting material is shown in Fig.1. Three cylindrical specimens with a diameter of 50 mm and a height of 100 mm were used for each curing age. The curing condition was in the arbitrary room temperature with no control, which was the same curing condition used for the cool pavements

Table 1 Chemical and physical properties

Properties	CWP	NZ
Chemical compositions (wt.%)		
SiO_2	70.90	70.15
Al_2O_3	21.10	12.28
Fe_2O_3	0.81	1.16
Cao	0.76	1.98
MgO	0.24	0.53
Na_2O	1.47	1.93
K_2O	3.57	2.38
TiO_2	0.33	0.17
MnO		0.06
Loss on ignition		9.25
Specific gravity	2.43	2.30
Specific surface area (cm^2/g)	1810	6770

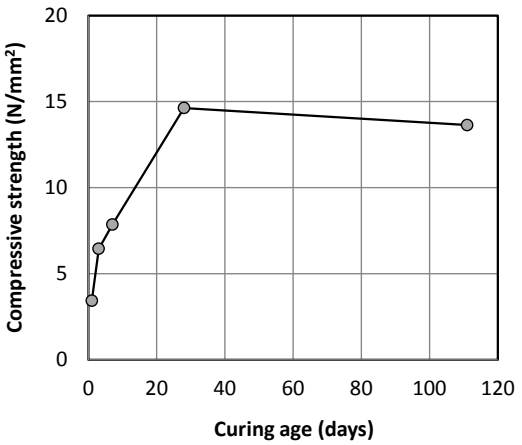

Fig.1 Compressive strength development of the cement-based grouting material

in the fatigue tests. The compressive strength grew up to 28 days and reached over 5 N/mm^2 in 3 days. The compressive strength over 5 N/mm^2 is recommended for the serviceability of the cool pavements on the traffic road. At 28 days, the compressive strength was 14.6 N/mm^2. The fatigue test for the asphalt pavement was started after the compressive strength became stable. The absorption ratio of the cement-based grouting material at the start of the fatigue test was 21.7%.

2.2 Specimens

The asphalt mixture used in this study was designed with a void ratio of 23% using straight asphalt bitumen with a 60/80 penetration and an addition of 3.5% bitumen by weight. The specimen has a square size of 650×650 mm and has a total thickness of 100 mm. The open graded asphalt pavement (porous asphalt pavement) with a thickness of 50 mm was paved on a hard rubber plate with a thickness of 50 mm as shown in Fig.2. The hard rubber plate has a hardness of 65±5, a Young's modulus of 3.42 N/mm^2, and a shear elastic modulus of 1.14 N/mm^2. The hard rubber plate with these properties was selected due to its deformability of the porous asphalt pavement as the plate behavior under the applied load.

Fig.2 Porous asphalt specimen after compaction

All the porous asphalt pavements were compacted using a roller compactor at the temperature of 150°C. After the temperature of the porous asphalt pavement decreased and the surface temperature reached 35°C, the cement-based grouting material was poured into the voids and vibrated on the surface as shown in Fig.3. Finally, the surface was treated with a rubber lake to keep it smooth. The porous asphalt pavements with and without the cement-based grouting material were prepared for each of the five specimens. In this paper, the specimen of the porous asphalt pavement is called PoAs and the specimen with

the cement-based grouting material is called JGZ.

Fig.3 Cement-based grouting material poured into voids of the porous asphalt specimen

2.3 Test method

The specimen placed in an aluminum mold was fixed in a water tank as shown in Fig.4 and was fully soaked in water at 40°C controlled by an electric heater. When the atmospheric temperature is 30°C in summer, the average temperature of the conventional asphalt pavement is about 40°C in depth [12]. In this test, the water temperature was thus determined as 40°C. The surface of the water tank was covered by styrene form plates except the loading plate area to prevent evaporation and temperature reduction of the water. After keeping the specimen in the 40°C water for 24 h, the fatigue test was started under the fixed-point load. The water level in the tank was kept constant during the fatigue test.

Fig.4 Specimen fixed in a water tank

The size of the loading steel plate was 150×60 mm, which is similar to the contact area (500×200 mm) of the rear tire having a design wheel load specified by Japanese Specifications for Roadway Bridges [13]. Then, the tire contact pressure is 1 N/mm^2. The maximum load applied was varied basically considering the contact pressure of 1 N/mm^2 as shown in Table 2. Also, the minimum load applied was kept at 0.5 kN. As the loading condition, a sine wave with a frequency of 3 Hz was applied in load control.

Table 2 Contact pressure applied to each specimen

PoAs	Contact pressure (N/mm^2)	JGZ	Contact pressure (N/mm^2)
PoAs-1	1.00	JGZ-1	1.10
PoAs-2	0.90	JGZ-2	1.00
PoAs-3	0.80	JGZ-3	0.95
PoAs-4	0.50	JGZ-4	0.90
PoAs-5	0.40	JGZ-5	0.80

The sinking displacement at the loading point was automatically measured at intervals by four linear variable-differential transducers (LVDTs) with a 25 mm capacity attached onto the corners of the loading plate as shown in Fig.5. The acquisition speed of the LVDTs was 1000 Hz so as to measure the maximum and minimum displacements with good accuracy under the repetitious loading. The interval of the data acquisition was 1 min for the PoAs specimens and 10 min for the JGZ specimens.

Fig.5 LVDTs attached onto the corners of the loading plate

In this test, the number of load cycles at fracture for the specimen was defined as the sinking displacement at both 15 mm and 20 mm. This value was considered due to the influence of rutting on the asphalt pavements. The standard maintenance strategies on the highway pavements against such rutting usually adopted the displacement of 15 mm or 20 mm according to the rutting maintenance level, water splash by vehicles, and hydroplaning phenomenon [14], [15]. In this

study, the specimen did not reach 20 mm in the fatigue tests, and the loading was stopped after 3 million load cycles.

3. RESULTS AND DISCUSSION

3.1 Fracture condition

After the fatigue tests, some specimens were cut by a concrete cutter to observe the permanent deformation and the injecting condition of the cement-based grouting material. For example, the fracture conditions of the cut PoAs-1 and JGZ-2 are shown in Fig.6. The loading position shifted downward due to decompressions caused by the breakdown of adhesion between the asphalt binder and the aggregates or the cement-based grouting material. Also, in the surrounding area of the loading position, upheavals appeared due to the lateral flow of asphalt mixture. From Fig.7, it can be confirmed that the cement-based grouting material filled the voids in the porous asphalt pavement.

(a) PoAs-1 specimen

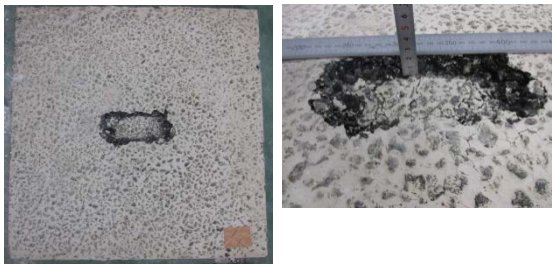

(b) JGZ-2 specimen

Fig.6 Observation of the fracture condition after cutting

Fig.7 Injecting condition of the cement-based grouting material in JGZ-3 specimen

3.2 Deflection behavior

The relationship between the sinking displacement at the loading point and the number of load cycles for each specimen is shown in Fig.8. The accelerated loading tests [5], [6] reported that the permanent deformation of asphalt mixtures is divided into three stages: 1) the initial stage of rapid compaction deformation by the loading, 2) the second stage of stable shear deformation due to shear stress, and 3) the third stage of the failure with the rapid increase of deformation. From Figs. 8(a) to (e), the deformation behavior of the PoAs specimens shows the stage 1) and 2). The displacement initially increased due to the compaction of the asphalt mixtures. After that, the behavior quickly changed to the stable deformation following a constant rate increase of the displacement. Before the rapid increase in the failure stage, the displacement reached over 20 mm. The number of load cycles with displacements of 15 mm and 20 mm are expressed in each figure. Figs.8(f) to (j) show the deformation behavior of the JGZ specimens. The displacement of the JGZ-1 specimen rapidly increased just after the loading. This is due to the data acquisition interval of a long-range as 10 min. The JGZ-1 and JGZ-2 reached over the targeted displacement of 20 mm. The JGZ-3 also reached over the targeted displacement of 15 mm. After that, however, the rate of the deformation speed became lower and the displacement did not reach 20 mm before 3 million load cycles. The JZG-4 and JGZ-5 showed lower displacement than the other specimens and behaved to increase stably up to 3 million load cycles. The results of the fatigue tests show that the deformation behavior significantly changed at the contact pressure around 0.95 N/mm^2.

As expected, when the loading level was higher, the deformation speed was higher and the number of load cycles up to the targeted displacement decreased. However, the JGZ specimens, in which the cement-based grouting material was poured into the voids, have the higher fatigue resistance and the lower shear deformation.

3.3 Fatigue life

From Figs.8(a) to (g), all the PoAs specimens and the JGZ-1 and the JGZ-2 specimens reached over the targeted displacement of 20 mm. In contrast, the JGZ-3 specimen did not reach over 20 mm. Hence, the number of load cycles at 20 mm in the JGZ-3 specimen was estimated by the linear approximation method as shown in Fig.9. The

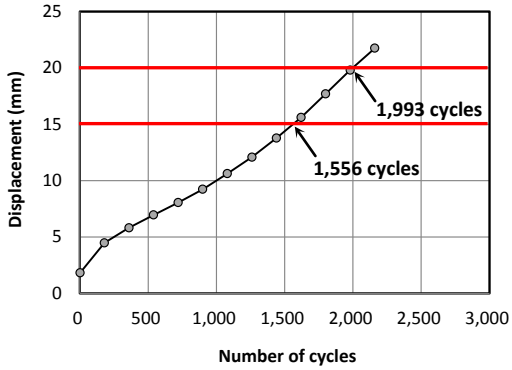

(a) PoAs-1 (Contact pressure 1.00 N/mm^2)

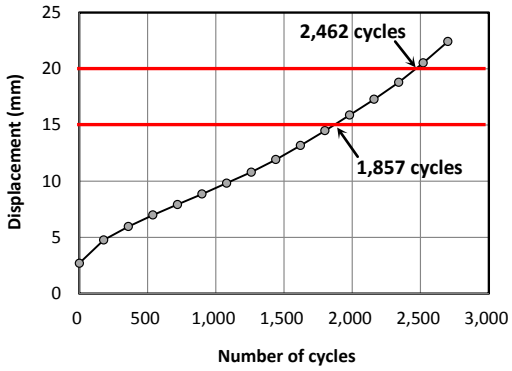

(b) PoAs-2 (Contact pressure 0.90 N/mm^2)

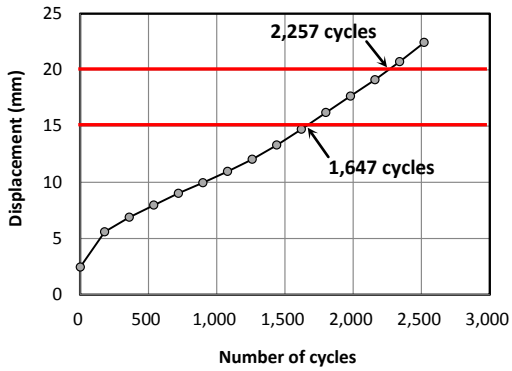

(c) PoAs-3 (Contact pressure 0.80 N/mm^2)

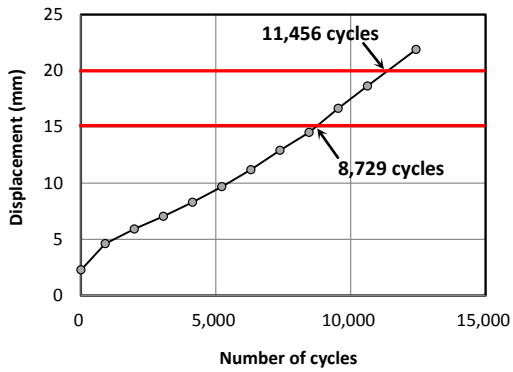

(d) PoAs-4 (Contact pressure 0.50 N/mm^2)

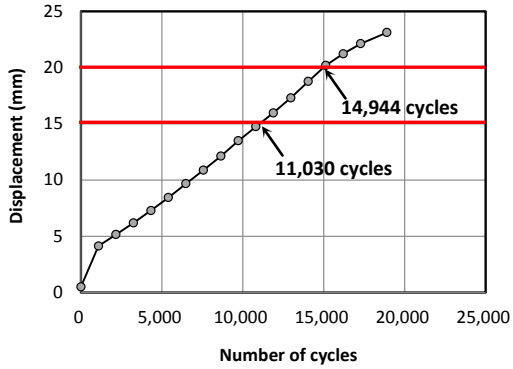

(e) PoAs-5 (Contact pressure 0.40 N/mm^2)

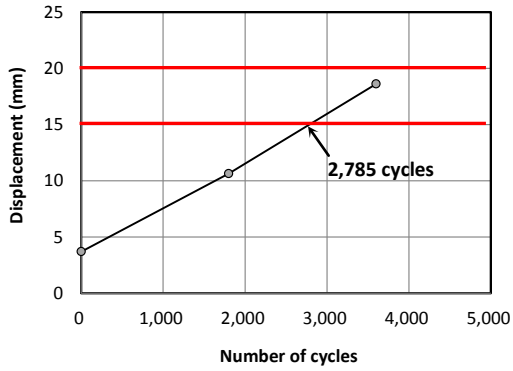

(f) JGZ-1 (Contact pressure 1.10 N/mm^2)

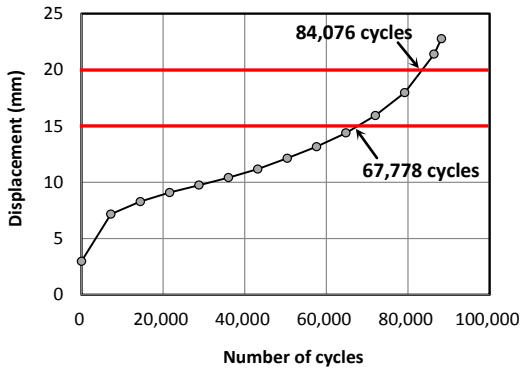

(g) JGZ-2 (Contact pressure 1.00 N/mm^2)

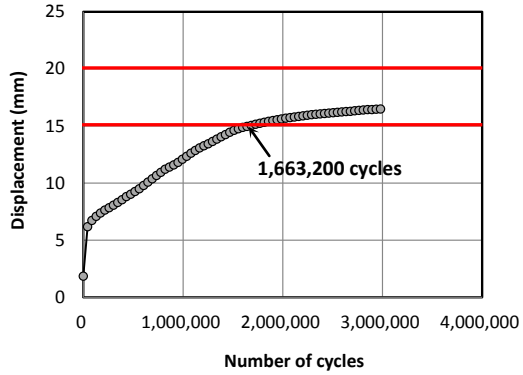

(h) JGZ-3 (Contact pressure 0.95 N/mm^2)

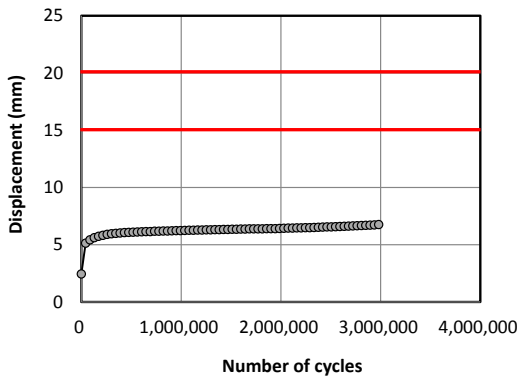

(i) JGZ-4 (Contact pressure 0.90 N/mm^2)

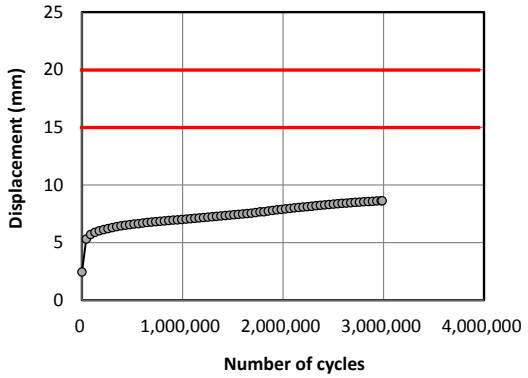

(j) JGZ-5 (Contact pressure 0.80 N/mm^2)

Fig.8 Sinking displacement at the loading position and the number of load cycles

number of load cycles at the displacements of 15 mm and 20 mm are listed in Table 3 for the PoAs specimens and Table 4 for the JGZ specimens.

Unfortunately, for the JGZ-4 and the JGZ-5, each displacement was quite lower to estimate the number of load cycles at the targeted displacements of 15 mm and 20 mm. Therefore, both these specimens were excluded from the comparison for the fatigue life.

From the fatigue life shown in Tables 3 and 4, the relationship between the contact pressure and the number of load cycles is plotted in the S-N diagram at each targeted displacement as shown in Fig.10. It can be seen that the data points are linearly plotted in each S-N diagram and the lower contact pressure is the higher fatigue life in the JGZ pavement in comparison with the PoAs pavements. Considering the actual contact pressure from the vehicle tire, the JGZ pavement has a greatly higher fatigue life than the porous asphalt pavement. Those S-N curves can be expressed as follows.

For the targeted displacement of 15 mm,
Porous asphalt pavement:

$$\log N = -1.569\sigma + 4.662 \quad (1)$$

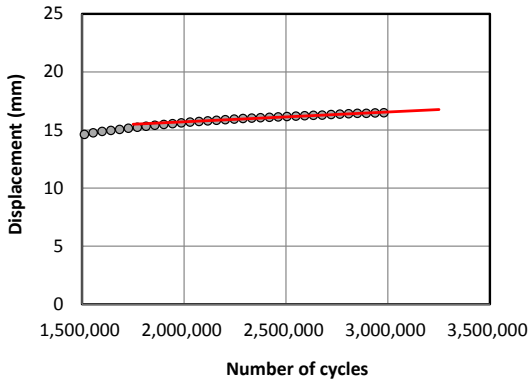

Fig.9 Linear approximation for the number of load cycles at 20 mm in the JGZ-3 specimen

Table 3 Fatigue life of PoAs specimens at each sinking displacement

Specimen	Contact pressure (N/mm^2)	Fatigue life (cycles) 15 mm	20 mm
PoAs-1	1.00	1,566	1,993
PoAs-2	0.90	1,857	2,462
PoAs-3	0.80	1,647	2,257
PoAs-4	0.50	8,729	11,456
PoAs-5	0.40	11,030	149,44

Table 4 Fatigue life of JGZ specimens at each sinking displacement

Specimen	Contact pressure (N/mm^2)	Fatigue life (cycles) 15 mm	20 mm
JGZ-1	1.10	2,785	3,913
JGZ-2	1.00	67,778	84,076
JGZ-3	0.95	1,663,200	7,120,796*
JGZ-4	0.90	–	–
JGZ-5	0.80	–	–

*The number of load cycles estimated by liner approximation.

JGZ pavement:

$$\log N = -17.844\sigma + 22.974 \quad (2)$$

For the targeted displacement of 20 mm,
Porous asphalt pavement:

$$\log N = -1.590\sigma + 4.807 \quad (3)$$

JGZ pavement:

$$\log N = -20.532\sigma + 25.997 \quad (4)$$

where, σ is the contact pressure (N/mm^2).

At the contact pressure of 1.0 N/mm^2, which is the rear tire contact pressure specified by Japanese Specifications for Roadway Bridges [13], the fatigue life of the JGZ pavement is about 40 times longer than that of the porous asphalt pavement.

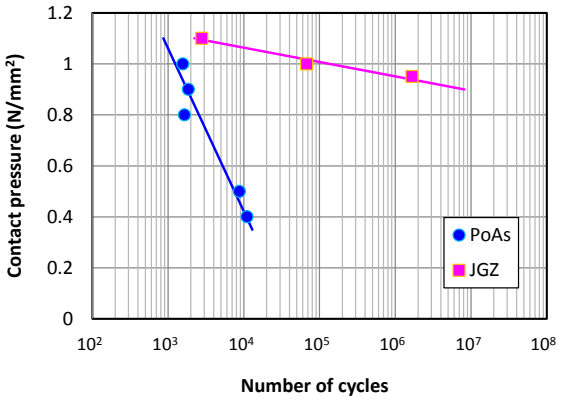

(a) Fatigue life at the sinking displacement of 15 mm

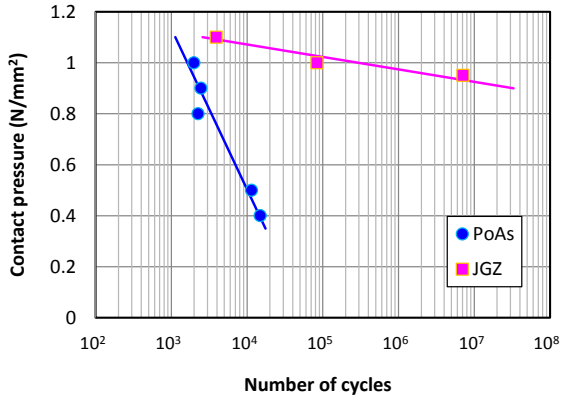

(b) Fatigue life at the sinking displacement of 20 mm

Fig.9 Contact pressure and fatigue life

From the results of the previous and present studies, it can be said that the JGZ pavement has the surface temperature reducing function and the higher fatigue resistance in comparison with the conventional porous asphalt pavement.

4. CONCLUSIONS

In this study, the fatigue tests under the fixed-point load were carried out to evaluate the fatigue life of the surface temperature reducing pavement developed by the authors. The main conclusions are as follows:

(1) In water at 40°C, the displacement at the loading point in the porous asphalt pavements rapidly increased up to the targeted displacement.

(2) The surface temperature reducing pavements, JGZ pavements, have a better deformation behavior than the porous asphalt pavements. At the contact pressure lower than 0.95 N/mm^2, the deformation behavior increased gradually and did not reach the targeted displacement before 3 million load cycles.

(3) For both the targeted displacements of 15 mm and 20 mm, the fatigue life can be represented by the S-N curve for each pavement. This suggests that the surface temperature reducing pavement has considerably higher resistance to the fatigue in water at 40°C. In the future research work, the fatigue tests of the surface temperature reducing pavement will be conducted with different water temperatures.

5. ACKNOWLEDGEMENTS

The first author wishes to acknowledge the financial support of JSPS KAKENHI (Grant Number JP 16K06451), Japan. The authors are also grateful to BASF Japan Ltd. for supplying the chemical admixture.

6. REFERENCES

[1] Santamouris M, “Using cool pavements as a mitigation strategy to fight urban heat island-A review of the actual developments”, Renewable and Sustainable Energy Reviews, Vol. 26, 2013, pp. 224-240.

[2] Qin Y, “A review on the development of cool pavements to mitigate urban heat island effect”, Renewable and Sustainable Energy Reviews, Vol. 52, 2015, pp. 445-459.

[3] Higashiyama H, Sano S, Nakanishi F, Takahashi O, Tsukuma S, “Field measurements of road surface temperature of several asphalt pavements with temperature rise reducing function”, Case Studies in Construction Materials, Vol. 4, 2016, pp. 73-80.

[4] Higashiyama H, Sano S, Nakanishi F, Sugiyama M, Takahashi O, Tsukuma S, “Effect on surface temperature reduction of asphalt pavements with cement-based grouting materials containing ceramic waste powder”, Int. J. of Civil, Environment, Structural, Construction and Architecture Engineering, Vol. 10, No. 8, 2016, pp. 1014-1020.

[5] Zhou F, Scullion T, Sun L, “Verification and modeling of three-stage permanent deformation behavior of asphalt mixes”, J. of Transportation Engineering, ASCE, Vo. 130, No. 4, 2004, pp. 486-494.

[6] Xu Y, Sun L, “Study on permanent deformation of asphalt mixes by single penetration repeated shear test”, Procedia-

Social and Behavioral Sciences, Vol. 96, 2013, pp. 886-893.

[7] Cooper SB, Mohammad LN, Elseifi MA, "Laboratory performance characteristics of sulphur-modified warm-mix asphalt", J. of Materials in Civil Engineering, Vol. 23, No. 9, 2011, pp. 1338-1345.

[8] Goh SW, You Z, "Evaluation of warm mix asphalt produced at various temperatures through dynamic modulus testing and four point beam fatigue testing", in Proc. The GeoHunan Int. Conference-pavements and materials: recent advances in design, testing, and construction, Hunan China: Geotechnical Special Publication 212, 2011, pp. 123-130.

[9] Sanchez-Alonso E, Vega-Zamanillo A, Calzada-Perez AC, Castro-Fresno D, "Effect of warm additives on rutting and fatigue behavior of asphalt mixtures", Construction and Building Materials, Vol. 47, 2013, pp. 240-244.

[10] Su K, Maekawa R, Hachiya Y, "Laboratory evaluation of WMA mixture for use in airport pavement rehabilitation", Construction and Building Materials, Vol. 23, 2009, pp. 2709-2714.

[11] Japan Society of Civil Engineers, "Test method for flowability of grout mortar for prepacked concrete (P-type funnel method), JSCE-F 521-1999", Standard Specifications for Concrete Structures, Test Methods and Specifications, 2005, p. 209 (in Japanese).

[12] Japan Road Association, "Design Handbook for Pavements", 2006 (in Japanese).

[13] Japan Road Association, "Japanese Specifications for Roadway Bridges", 2012 (in Japanese).

[14] Kubo K, "Rational maintenance of the pavement of national highways", Construction Execution Project, No. 684, 2007, pp. 6-10 (in Japanese).

[15] Abe Y, Iino T, "A study on the numerical analysis of rutting depth data", J. of Japan Society of Civil Engineers, No.478/V-21, 1993, pp. 117-123 (in Japanese).